Supplemental Material

The allosteric regulatory mechanism of the E. coli MetNI methionine ABC transporter

Janet G. Yang and Douglas C. Rees

Figures S1-S3

Table S1

Modeling of MetNI inhibition

Figure S1

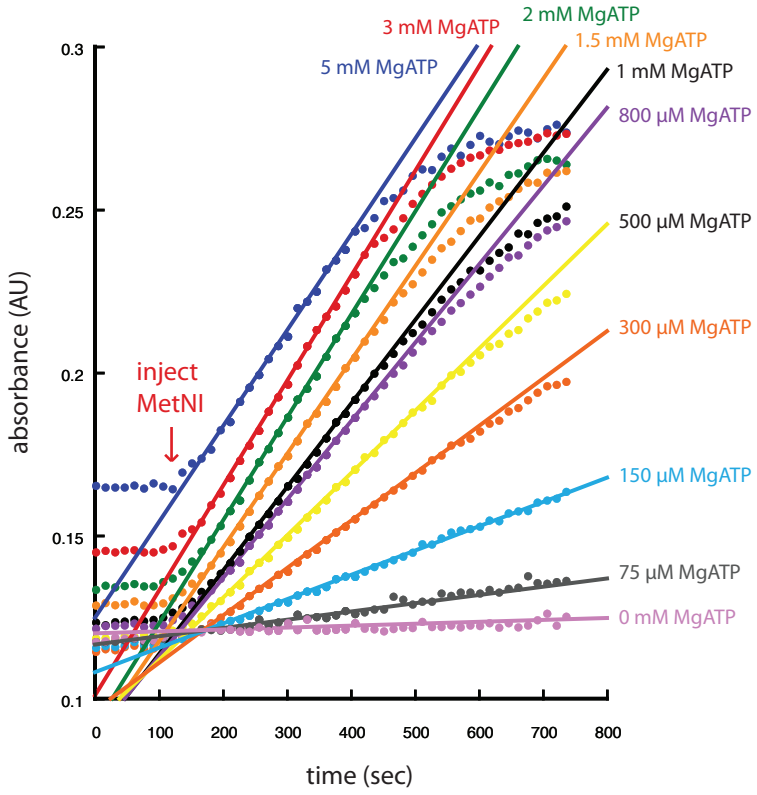

Figure S1. Representative raw data for ATPase assays. The amount of inorganic phosphate generated in solution was measured in real-time using the Enzchek Phosphate Assay Kit (Molecular Probes). Each 100 µl reaction contained 60 mM Tris, pH 7.5, 5 mM TAPS, pH 8.5, 0.055% DDM, 55 mM NaCl, 200 µM 2-amino-6-mercapto-7-methylpurine riboside, 0.1 units of purine nucleoside phosphorylase, equimolar amounts of $MgCl_2$ and ATP. Data were collected on an Infinite M200 microplate reader (Tecan Group) at 33°C. Reactions were incubated for 2 minutes and then initiated by automatic injection of MetNI to a final concentration of 410 nM. Initial rates were obtained by calculating the linear portion of the change (200-400 sec) in absorbance at 360 nm as a function of time.

Figure S2

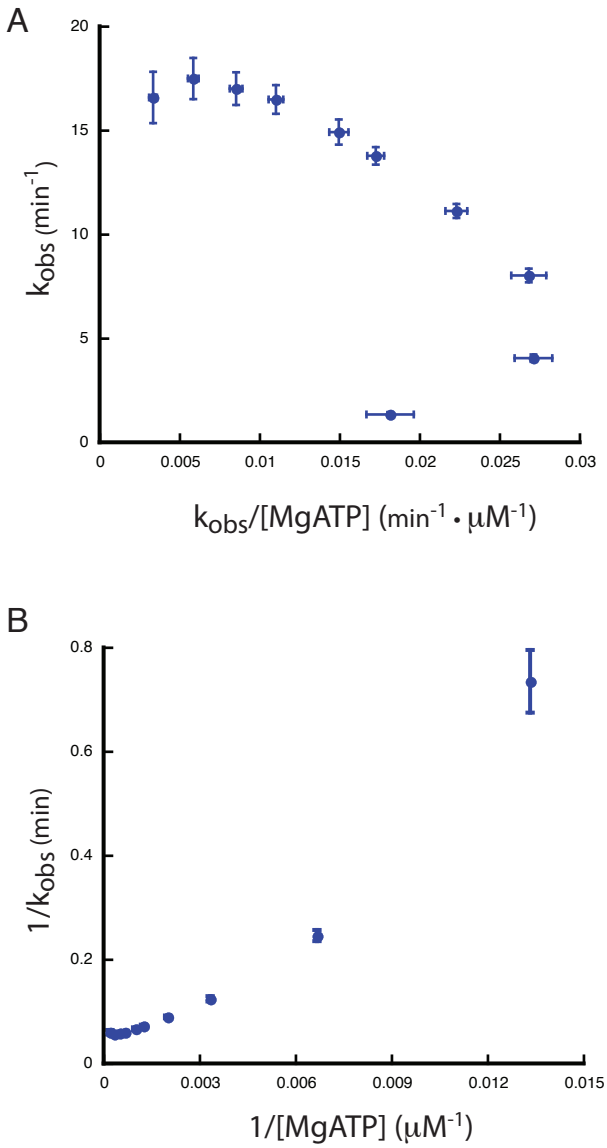

Figure S2. Graphical representations of positive cooperativity for MgATP. Data from Figure 1C replotted as (A) Eadie-Hofstee plot and (B) Lineweaver-Burk plot.

Figure S3

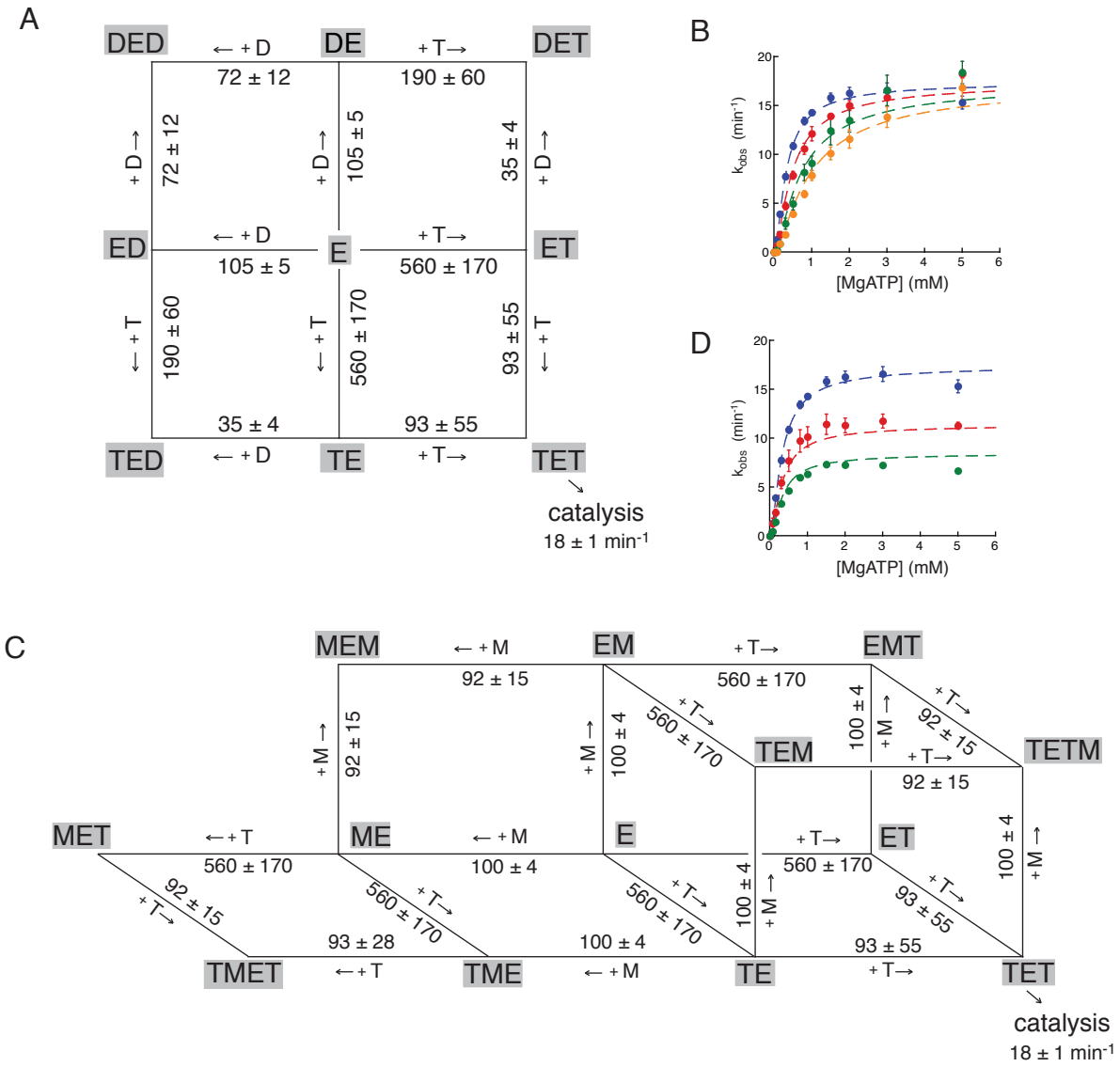

Figure S3. Theoretical models for competitive and noncompetitive inhibition. All values represent intrinsic dissociation constants. A, Thermodynamic scheme for competitive inhibition by ADP. MetNI is represented by "E"; ATP by "T", and ADP by "D". B, Fit of ADP data using model depicted in (A). Blue, no ADP; red, 30 μM ADP; green, 75 μM ADP; yellow, 120 μM ADP. C, Thermodynamic scheme for noncompetitive inhibition by L-methionine. MetNI is represented by "E"; ATP by "T", and L-met by "M". D, Fit of L-met data using model depicted in (C). Blue, no L-met; red, 25 μM L-met; green, 50 μM L-met.

Modeling of MetNI inhibition

Using the kinetic data, we generated several models to quantitatively test different thermodynamic schemes for inhibition. Nonlinear regression analysis was performed using Mathematica's NonlinearModelFit function. Equations for fitting were derived as per Segel (see below) (1).

All models require the binding of two ATP molecules per transporter for hydrolysis, as supported by the cooperativity observed in Fig 1B. Additionally, crystallographic studies of ABC subunits suggest that two bound ATP molecules are needed to stabilize the interface between the TMDs (2,3). While ATP hydrolysis may occur with only 1 bound ATP, as suggested by the Hill coefficient of 1.7, we chose to not include this species in our modeling studies to minimize the number of refined parameters. For ADP inhibition, the data best fit a model where one MetNI transporter ("E") can bind one molecule of ATP ("T") and one molecule of ADP ("D") simultaneously (Fig S3, A-B and Table S1). The presence of the mixed state, DET and TED, is not unexpected; it is conceivable that MetNI could hydrolyze only one ATP at a time, although this condition was not required to fit the kinetic model. The doubly bound DED state has been observed crystallographically in an inward facing conformation (4). More detailed comparisons of binding affinities were difficult to infer due to the large standard errors, a consequence of the highly correlative nature of the model parameters (5).

The model for L-methionine inhibition is more complicated, as there are two binding sites for ATP and two allosteric binding sites for L-methionine ("M") per one transporter (Fig S3, C-D and Table S1). The data best fit a model in which only one species is able to hydrolyze ATP. The single catalytically active species contains to two ATP and no L-methionine (TET) and represents ~24% of the population at intracellular concentrations of 150 μM L-met and 9.6 mM ATP (6). Conversely, when MetNI is bound to two ATP and one L-methionine, TEMT and TMET, hydrolysis cannot occur (~74% of population). Intriguingly, we found that the presence of one bound L-methionine does not affect the binding affinity of either the first or second molecule of ATP. For example, the binding affinity for $E + T \rightarrow ET$ is the same as that of $EM + T \rightarrow EMT$. Cooperative binding for ATP is maintained as well: $ET + T \rightarrow TET$ is the same as that for $EMT + T \rightarrow TEMT$. These two observations suggest that the binding of one methionine may not induce a substantial enough conformational change at the NBD interface to affect nucleotide binding, and yet is able to disrupt catalysis.

Derivation of basic equations for global modeling

An ATPase reaction for a unireactant system can be visualized as:

$$E + S \overset{K_S}{\rightleftharpoons} ES \overset{k_{cat}}{\longrightarrow} E + P$$

The Michaelis-Menten equation can be used to describe the ATPase reaction under rapid equilibrium conditions:

$$v = k_{cat} * \frac{[E]_t\,[S]}{K_S + [S]} = V_{max} * \frac{[S]}{K_S + [S]}$$

where v is the initial velocity, $[S]$ is a fixed ATP concentration, $[E]_t$ is the total concentration of enzyme, k_{cat} is the catalytic rate constant, and K_S is the dissociation constant for the ATP bound enzyme.

This can be rewritten in an alternate form:

$$\frac{v}{[E]_t} = k_{obs} = k_{cat} * \frac{\frac{[S]}{K_s}}{1 + \frac{[S]}{K_S}}$$

where k_{obs} is the observed rate constant. In this form, the numerator contains only one term, indicating that there exists only one product forming species. There are two terms in the denominator, indicating that there are a total of two species, free E and ES complex.

Derivation of basic equations, continued

In the presence of an inhibitor, the Michaelis-Menten equation includes an additional term for the enzyme-inhibitor complex:

$$v = k_{cat} * \frac{[E]_t [S]}{K_S \left(1 + \frac{[I]}{K_I}\right) + [S]}$$

where [I] is a fixed concentration of inhibitor, and K_I is the dissociation constant for the inhibitor bound enzyme.

This can be rewritten in an alternate form:

$$k_{obs} = k_{cat} * \frac{\frac{[S]}{K_S}}{1 + \frac{[S]}{K_S} + \frac{[I]}{K_I}}$$

Modeling of ADP inhibition data:

1. To obtain values for K_T, a, k_{cat} in the global model, we first fit the data (k_{obs} as a function of [ATP]) in the absence of inhibitor (data points shown in Figure 1c). Based on the Hill coefficient discussed in the main text, we assume that only the doubly ATP bound species can hydrolyze ATP (shown in the numerator). Thus the model presented here differs from that from the main text, since here it explicitly depends on T^2, while the equations in the main text are dependent on T^{nH}. There are a total of three possible species of enzyme, enzyme alone, singly bound by ATP, and doubly bound by ATP (represented in the denominator). If the identical ATP binding sites are cooperative, the binding of one molecule of ATP can alter the intrinsic dissociation constant of the vacant ATP site by the factor "a". When the value of "a" is between 0 and 1, the binding of ATP exhibits positive cooperativity. The equation is as follows:

$$k_{obs} = k_{cat} * \frac{\frac{T^2}{aK_T^2}}{1 + \frac{2T}{K_T} + \frac{T^2}{aK_T^2}}$$

where

T — [ATP]

K_T — intrinsic dissociation constant for ATP

a — interaction factor for binding of second ATP

k_{cat} — catalytic rate constant

Parameter estimates are as follows:

K_T = 560 ± 160 μM

a = 0.17 ± 0.08

k_{cat} = 17.5 ± 0.5 min^{-1}

Modeling of ADP inhibition data, continued:

2. To obtain K_D and c for the global fit, we then fit the data observed at subsaturating, constant [ATP] and varying [ADP]. These data points are shown in Figure 2A.

$$k_{obs} = \frac{V_{max}^{app}}{1 + \frac{2D}{K_D} + \frac{D^2}{cK_D^2}}$$

where

V_{max}^{app} — apparent maximal velocity at subsaturating ATP

D — [ADP]

K_D — intrinsic dissociation constant for ADP

c — interaction factor for binding of second ADP

Parameter estimates are as follows:

K_D = 105 ± 5 μM

c = 0.68 ± 0.12

V_{max}^{app} = 0.85 ± 0.01 min^{-1}

Modeling of ADP inhibition data, continued:

3. From the parameter estimates obtained in Steps #1 and #2, we fixed the values for the following parameters:

$$K_T, a, K_{D,}\, c, k_{cat}$$

and globally fit the four data sets observed at constant [ADP] and varying [ATP] (data points shown in Figure 2b) using the following equation:

$$k_{obs} = k_{cat} * \frac{\frac{T^2}{aK_T^2}}{1 + \frac{2T}{K_T} + \frac{T^2}{aK_T^2} + \frac{2TD}{bK_TK_D} + \frac{2D}{K_D} + \frac{D^2}{cK_D^2}}$$

and fitting only one floating parameter:

b — interaction factor for binding of ATP with one bound ADP or binding of ADP with one bound ATP (these are thermodynamically equivalent)

The parameter estimate is as follows:

b = 0.34 ± 0.03

Modeling of L-Methionine inhibition data

4. To fix parameters K_I and d, we fit the data observed at saturating, constant [ATP] and varying [L-met] (data points show in Figure 3A).

$$k_{obs} = \frac{V_{max}}{1 + \frac{2I}{K_I} + \frac{I^2}{dK_I^2}}$$

where

I — [L-Methionine]

K_I — intrinsic dissociation constant for L-Met

d — interaction factor for binding of second L-Met

V_{max} — maximal velocity

Parameter estimates are as follows:

K_I = 100 ± 4 μM

d = 0.91 ± 0.15

V_{max} = 20.5 ± 0.16 min^{-1}

Modeling of L-Methionine inhibition data, continued

5. From the parameter estimates obtained in Steps #1 and #4, we fixed the values for the following parameters:

$$K_T, a, K_{I,}\, d, k_{cat}$$

and globally fit the four data sets observed at constant [L-met] and varying [ATP] (data points shown in Figure 3B) using the following equation:

$$k_{obs} = k_{cat} * \frac{\frac{T^2}{aK_T^2}}{1 + \frac{2T}{K_T} + \frac{T^2}{aK_T^2} + \frac{2I}{K_I} + \frac{I^2}{dK_I^2} + \frac{4TI}{eK_TK_I} + \frac{2T^2I}{fK_T^2K_I} + \frac{2TI^2}{gK_TK_I^2} + \frac{T^2I^2}{hK_T^2K_I^2}}$$

where

- e — interaction factor for binding of one ATP with one bound L-Met or binding of one L-Met with one bound ATP
- f — interaction factor for binding of second ATP with one bound L-Met and one bound ATP
- g — interaction factor for binding of second L-Met with one bound ATP and one bound L-Met
- h — interaction factor for binding of second ATP with two bound L-Met and one bound ATP, or binding of second L-Met with two bound ATP and one bound L-Met

6. We first chose to eliminate the doubly bound ATP, doubly bound L-Met species as this is the least likely to be physiologically relevant. The equation was simplified to:

$$k_{obs} = k_{cat} * \frac{\frac{T^2}{aK_T^2}}{1 + \frac{2T}{K_T} + \frac{T^2}{aK_T^2} + \frac{2I}{K_I} + \frac{I^2}{dK_I^2} + \frac{4TI}{eK_TK_I} + \frac{2T^2I}{fK_T^2K_I} + \frac{2TI^2}{gK_TK_I^2}}$$

Modeling of L-Methionine inhibition data, continued

7. Next, as f and g depend on e, we chose to focus on the e parameter. We fixed e at successive values and determined that the best fit was achieved when $e = 1$. The equation was further simplified to the following:

$$k_{obs} = k_{cat} * \frac{\frac{T^2}{aK_T^2}}{1 + \frac{2T}{K_T} + \frac{T^2}{aK_T^2} + \frac{2I}{K_I} + \frac{I^2}{dK_I^2} + \frac{4TI}{K_T K_I} + \frac{2T^2 I}{fK_T^2 K_I} + \frac{2TI^2}{gK_T K_I^2}}$$

8. There were several combinations of values for f and g that resulted in same goodness-of-fit.

9. We next tried to eliminate an additional species – either the doubly bound ATP, singly bound L-met species or the doubly bound L-met, singly bound ATP species. We were able to obtain a similar goodness-of-fit as Step #8 only when the doubly bound L-met, singly bound ATP species was eliminated. Thus the final equation for the global fitting is as follows:

$$k_{obs} = k_{cat} * \frac{\frac{T^2}{aK_T^2}}{1 + \frac{2T}{K_T} + \frac{T^2}{aK_T^2} + \frac{2I}{K_I} + \frac{I^2}{dK_I^2} + \frac{4TI}{K_T K_I} + \frac{2T^2 I}{fK_T^2 K_I}}$$

and fitting only one floating parameter:

f — interaction factor for binding of second ATP when one ATP and one L-Met are bound

The parameter estimate is as follows:

f = 0.16 ± 0.01

Modeling of L-Methionine inhibition data, continued

10. The goodness-of-fit in the above steps was measured using the following equation:

$$\% \, RMSD = \sqrt{\frac{\frac{\sum_{t=1}^{n}(k_{obs_t} - k_{mod_t})^2}{{k_{obs_t}}^2}}{n}}$$

where

n — number of average values from 3 independent experiments

k_{obs} — observed rate constant

k_{mod} — modeled rate constant

11. The % RMSD for the final fit (equation shown in Step #9) was 2.3%.

References

1. Segel, I. H. (1993) *Enzyme kinetics : behavior and analysis of rapid equilibrium and steady state enzyme systems*, Wiley, New York; Toronto
2. Korkhov, V. M., Mireku, S. A., Veprintsev, D. B., and Locher, K. P. (2014) Structure of AMP-PNP-bound BtuCD and mechanism of ATP-powered vitamin B12 transport by BtuCD-F. *Nat Struct Mol Biol* **21**, 1097-1099
3. Oldham, M. L., and Chen, J. (2011) Snapshots of the maltose transporter during ATP hydrolysis. *Proc Natl Acad Sci U S A* **108**, 15152-15156
4. Johnson, E., Nguyen, P. T., Yeates, T. O., and Rees, D. C. (2012) Inward facing conformations of the MetNI methionine ABC transporter: Implications for the mechanism of transinhibition. *Protein Sci* **21**, 84-96
5. Hines, K. E., Middendorf, T. R., and Aldrich, R. W. (2014) Determination of parameter identifiability in nonlinear biophysical models: A Bayesian approach. *J Gen Physiol* **143**, 401-416
6. Bennett, B. D., Kimball, E. H., Gao, M., Osterhout, R., Van Dien, S. J., and Rabinowitz, J. D. (2009) Absolute metabolite concentrations and implied enzyme active site occupancy in *Escherichia coli*. *Nat Chem Biol* **5**, 593-599

Table S1. Intrinsic dissociation constants

Constant	Description	Value (μM)
$K_D^{apo \rightarrow ATP}$	apo MetNI binds one ATP	560 ± 170
$K_D^{ATP \rightarrow ATP*}$	ATP-MetNI binds second ATP	93 ± 55
$K_D^{apo \rightarrow ADP}$	Apo MetNI binds one ADP	110 ± 10
$K_D^{ADP \rightarrow ADP}$	ADP-MetNI binds second ADP	72 ± 12
$K_D^{ATP \rightarrow ADP}$	ATP-MetNI binds one ADP	35 ± 4
$K_D^{ADP \rightarrow ATP}$	ADP-MetNI binds one ATP	190 ± 60
$K_D^{apo \rightarrow Met}$	Apo MetNI binds one Met	100 ± 4
$K_D^{Met \rightarrow Met}$	Met-MetNI binds second Met	92 ± 15
$K_D^{Met \rightarrow ATP}$	Met-MetNI binds one ATP	560 ± 170
$K_D^{ATP \rightarrow Met}$	ATP-MetNI binds one Met	100 ± 4
$K_D^{ATP/Met \rightarrow ATP}$	ATP-Met-MetNI binds second ATP	92 ± 28

*$k_{cat} = 18 \pm 1\ min^{-1}$ in the presence of two ATPs

The above intrinsic dissociation constants are defined in terms of binding to a single site (rather than a single molecule of MetNI). Numerical differences in constants between these values and those in the main text are due to differences in equations used for fitting, as described in Step #1.